Comparison of Digital Control Techniques for Low Cost UPS Applications

Cassiano Rech, Humberto Pinheiro, Hélio L. Hey, Hilton A. Gründling and José R. Pinheiro

Power Electronics and Control Research Group – GEPOC
Federal University of Santa Maria – UFSM
97105-900 – Santa Maria, RS – Brazil
cassiano@ieee.org, renes@ctlab.ufsm.br - http://www.ufsm.br/gepoc

***Abstract* – This paper presents a comparison among digital control techniques with repetitive integral action suitable to uninterruptible power supplies. As a result of the repetitive action, these digital control schemes can reduce the steady-state error and distortions caused by unknown periodic disturbances usually resulted from the input source and output load. Moreover, these digital control schemes measure only the output voltage, decreasing the amount of sensors and, consequently, the overall system cost. The control laws, stability analysis, common and distinguishing features of these control algorithms are discussed. Experimental results from a PWM inverter (110 V_{RMS}, 1 kVA) controlled by a low cost microcontroller are presented to demonstrate the control techniques performance under different load conditions, output filters and command strategy.**

I. INTRODUCTION

The widespread availability of low cost microcontrollers and DSP processors has made possible the increasingly use of these components for real-time control of static converters. The possibility to include as many of the control functions as possible in software, thereby increasing reliability and reducing costs, makes the digital control of uninterruptible power supply (UPS) systems commercially attractive. Digital control techniques should generate the pulse width modulated (PWM) signal to produce the sinusoidal output voltage of the UPS system with low total harmonic distortion (THD) for linear and nonlinear loads [1], [2]. Nevertheless, although these techniques present satisfactory results for load transients, the output voltage waveform normally presents high THD for nonlinear cyclic loads, such as ac phase-controlled loads and rectifier loads.

Repetitive control theory provides an alternative to minimize periodic errors that can occur in a dynamic system [3]. The repetitive action improves the steady-state response of a control system when the reference input signal and disturbances are periodic, consisting of harmonic components of a common fundamental frequency. Several repetitive control schemes have been developed and applied to minimize the steady-state error and periodic distortions that can appear in single-phase PWM inverters [4]–[10].

Although many digital control schemes have been developed for UPS applications in the last years, most of the published work has concentrated on the control law and supposed advantages of the specific control scheme, rather than on providing an in depth analysis of the overall control system. It is therefore the aim of this paper to provide a comparison among digital control techniques with repetitive integral action applied to low power (500 VA – 5 kVA) UPS systems. The digital control techniques analyzed are: predictive OSAP (One Sampling Ahead Preview) controller, predictive PID (proportional-integral-derivative) controller with a feedforward action, and model reference controller. The digital control schemes considered measure only the output voltage, decreasing the amount of sensors and, consequently, the overall system cost. The control laws, stability analysis, and simulation and experimental results are presented to demonstrate the main features of these digital control schemes. Common and distinguishing features are identified, and system performance analyzed in terms of these features.

This paper is organized as follows. Section II describes the plant model and analyzes the effects of increasing the PWM inverter switching frequency. The predictive OSAP controller with repetitive integral action is described in Section III. Section IV presents the predictive PD-feedforward control law with repetitive controller. The model reference controller with repetitive integral action is presented in Section V. Section VI gives the stability analysis of the closed-loop systems with the controllers of previous sections. Section VII shows a comparison of the simulation results, and Section VIII presents experimental results obtained for linear and nonlinear loads based on a microcontroller-controlled system.

II. PLANT MODEL

A typical single-phase PWM inverter is shown in Fig. 1, where the full-bridge inverter, LC filter and resistive load *R* are considered as the plant to be controlled. A Triac connected in series with a resistive load or a full-bridge rectifier with RC filter can be used to evaluate the performance of the system with nonlinear loads.

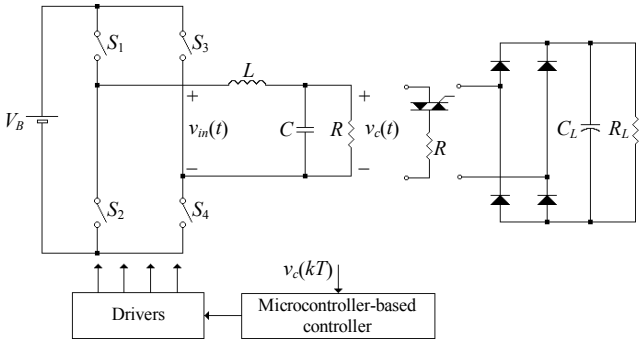

Fig. 1. Digitally controlled PWM inverter.

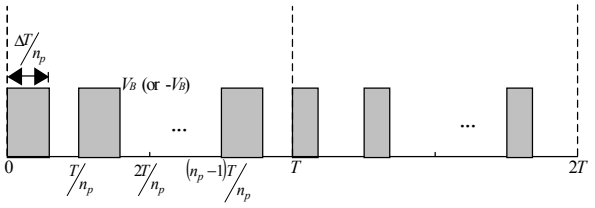

Fig. 2. PWM pattern.

The power circuit shown in Fig. 1 is modeled as a second-order system with the state vector $\left[v_c(t) \quad \dot{v}_c(t)\right]^T$, where $v_c(t)$ is the output voltage and $\dot{v}_c(t)$ is the derivative of $v_c(t)$. As a result, the state equation and the output equation are:

$$\begin{aligned} \dot{\mathbf{x}}(t) &= \mathbf{A}\mathbf{x}(t) + \mathbf{B}v_{in}(t) \\ y(t) &= \mathbf{C}\mathbf{x}(t) \end{aligned} \tag{1}$$

where

$$\mathbf{x}(t) = \begin{bmatrix} v_c(t) \\ \dot{v}_c(t) \end{bmatrix},\ \mathbf{A} = \begin{bmatrix} 0 & 1 \\ -\omega_p^2 & -2\zeta_p\omega_p \end{bmatrix},\ \mathbf{B} = \begin{bmatrix} 0 \\ \omega_p^2 \end{bmatrix},$$
$$\mathbf{C} = \begin{bmatrix} 1 & 0 \end{bmatrix},\ \omega_p = \frac{1}{\sqrt{LC}},\ \zeta_p = \frac{1}{2R}\sqrt{\frac{L}{C}} \tag{2}$$

It is well known that increasing the switching frequency of the PWM inverter it is possible to reduce the parameters of the output filter and possibly improve the dynamic response of the system. However, due to the computation time of the control law, it is not possible to increase the sampling frequency (updating frequency of the control law) at the same rate. In this way, the switching frequency can be increased while the sampling frequency is maintained the same, as shown in Fig. 2. With this PWM pattern, which may be called of MPWM (Multi-Pulse Width Modulation) pattern, the switching devices are turned on and off n_p times during each sampling interval T so that the inverter voltage $v_{in}(t)$ becomes n_p pulses of magnitude $+V_B$ or $-V_B$, and width $\Delta T/n_p$.

Therefore, the sampled-data equation of the system can be obtained solving (1) in a sampling period, that is:

$$\begin{aligned} \mathbf{x}(k+1) = e^{\mathbf{A}T}\mathbf{x}(k) &+ \int_0^{\frac{\Delta T(k)}{n_p}} e^{\mathbf{A}(T-\tau)}\mathbf{B}V_B d\tau + \\ &+ \int_{\frac{T}{n_p}}^{\frac{T+\Delta T(k)}{n_p}} e^{\mathbf{A}(T-\tau)}\mathbf{B}V_B d\tau + \ldots + \int_{\frac{(n_p-1)T}{n_p}}^{\frac{(n_p-1)T+\Delta T(k)}{n_p}} e^{\mathbf{A}(T-\tau)}\mathbf{B}V_B d\tau \end{aligned} \tag{3}$$

In this way, the nonlinear discrete-time state equation can be obtained solving (3):

$$\mathbf{x}(k+1) = e^{\mathbf{A}T}\mathbf{x}(k) + \left(\sum_{i=1}^{n_p} e^{\frac{i\mathbf{A}T}{n_p}}\right)\mathbf{A}^{-1}\left(\mathbf{I} - e^{\frac{-\mathbf{A}\Delta T(k)}{n_p}}\right)\mathbf{B}V_B \tag{4}$$

Considering that $e^{-\mathbf{A}\Delta T(k)/n_p}$ can be computed by using Taylor series, it is possible to obtain a linear discrete model from (4) by neglecting terms of higher than ΔT^2, that is:

$$\mathbf{x}(k+1) = \begin{bmatrix} g_{11} & g_{12} \\ g_{21} & g_{22} \end{bmatrix}\mathbf{x}(k) + \begin{bmatrix} h_1 \\ h_2 \end{bmatrix}\Delta T(k) \tag{5}$$

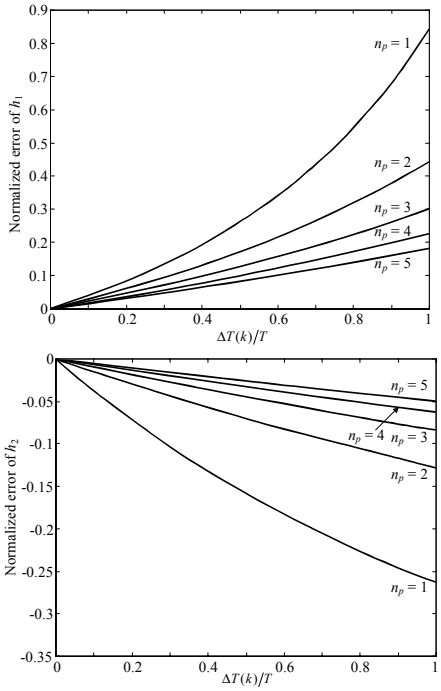

Fig. 3. Modeling errors for different values of n_p (ω_p = 1155 rad/s, ζ_p = 0.24).

or, in a compact form:

$$\mathbf{x}(k+1) = \mathbf{G}\,\mathbf{x}(k) + \mathbf{H}\,\Delta T(k) \tag{6}$$

where

g_{ij} is the corresponding element of $\mathbf{G} = e^{\mathbf{A}T}$, and

h_i is the corresponding element of $\mathbf{H} = \frac{1}{n_p}\left(\sum_{i=1}^{n_p} e^{i\mathbf{A}T/n_p}\right)\mathbf{B}V_B$.

However, due to the linearization of the nonlinear discrete-time plant model (4), the parameters of the input matrix **H** are different from the real ones. Fig. 3 shows the normalized errors, where the respective parameter of the nonlinear model is used as base value, between the parameters of the input matrix **H** (h_1 and h_2) and respective parameters of the nonlinear model, for different values of voltage pulses per sampling period (n_p). It can be clearly seen that the modeling errors caused by the linearization are reduced, increasing only the switching frequency of the PWM inverter [8].

From a linear discrete-time plant model, the input-output representation of (5) in the z-domain can be obtained:

$$y(z) = \frac{h_1 + (h_2 g_{12} - h_1 g_{22})z^{-1}}{z - (g_{11} + g_{22}) + (g_{11}g_{22} - g_{12}g_{21})z^{-1}}\Delta T(z) \tag{7}$$

Hence, the following difference equation can be obtained:

$$y(k+1) + a_1 y(k) + a_2 y(k-1) = b_1 u(k) + b_2 u(k-1) \tag{8}$$

where the input variable and the gains of the equation are:

$$\begin{aligned} u(k) &= \frac{\Delta T(k)}{T}V_B & b_1 &= h_1\,T/V_B \\ a_1 &= -(g_{11} + g_{22}) & b_2 &= (h_2 g_{12} - h_1 g_{22})T/V_B \\ a_2 &= g_{11}g_{22} - g_{12}g_{21} \end{aligned} \tag{9}$$

III. Predictive OSAP Controller with Repetitive Integral Action

The OSAP controller is a deadbeat control law that uses only one voltage sensor [1]. Thus, the cost of the overall system and the computation time of the controller are reduced. The OSAP control law can be obtained from (8) considering that the output is equal to the reference signal at the next sampling instant, then $y(k+1)$ can be substituted by $r(k+1)$. Then, the following control law can be obtained:

$$u_{OSAP}(k)=\frac{r(k+1)+p_1y(k)+p_2y(k-1)-q_2u(k-1)}{q_1} \quad (10)$$

If the OSAP controller gains p_1, p_2, q_1 and q_2 are equal to the plant parameters a_1, a_2, b_1 and b_2, respectively, it becomes a deadbeat control law which forces the output voltage to be equal to the reference signal at the next sampling interval. However, if the plant parameters change after the controller gains in (10) have been determined, then the deadbeat response is no longer obtained [1].

Moreover, the pulse width determination for k-th sampling interval is started at $t = kT$ with the acquisition of the output voltage and then after the computation time the pulse width is determined. Consequently, the delay time caused by the output voltage analog-to-digital (A/D) conversion and control law computation reduces the maximum available pulse width.

To solve this problem, Nishida and Haneyoshi presented a predictive OSAP controller [5]. This control law can be found by using (8) to obtain $y(k)$, and substituting in (10), then:

$$u_{OSAP}(k)=\frac{r(k+1)+P_1y(k-1)+P_2y(k-2)-Q_2u(k-1)-Q_3u(k-2)}{Q_1} \quad (11)$$

where P_1, P_2, Q_1, Q_2 and Q_3 are the controller gains, given by:

$$\begin{aligned} P_1&=-\left(g_{11}^2+g_{11}g_{22}+g_{12}g_{21}+g_{22}^2\right)\\ P_2&=-\left(g_{11}g_{12}g_{21}-g_{11}^2g_{22}+g_{12}g_{21}g_{22}-g_{11}g_{22}^2\right)\\ Q_1&=h_1T/V_B\\ Q_2&=\left(h_1g_{11}+h_2g_{12}\right)T/V_B\\ Q_3&=\left(-h_1\left(g_{11}g_{22}+g_{22}^2\right)+h_2\left(g_{11}g_{12}+g_{12}g_{22}\right)\right)T/V_B \end{aligned} \quad (12)$$

Equation (11) shows that the required signals for the determination of the control law are the output voltage at the previous sampling instants ($y(k-1)$ and $y(k-2)$), the values of the control law at the previous sampling instants ($u(k-1)$ and $u(k-2)$), and the reference signal at the next sampling instant ($r(k+1)$). Hence, the pulse width computation can be completed during the previous sampling period, and the pulse width can be extended to the entire period T.

In addition, a repetitive controller can be added to the predictive OSAP controller, as shown in Fig. 4, to reduce the steady-state error and distortions caused by periodic disturbances, such as nonlinear loads [5]. The repetitive control law with an integral action can be written as:

$$u_{RP}(k)=c_1\sum_{i=1}^{\infty}e(k+N-in) \quad (13)$$

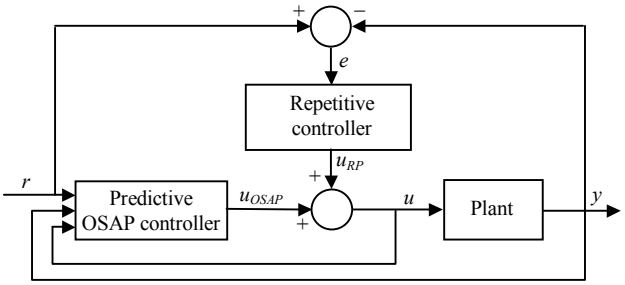

Fig. 4. Block diagram of the control system with OSAP-RP controller.

where $e(k) = r(k) - y(k)$ is the output error, c_1 is the gain of the repetitive controller, N is the time advance step size and n is the number of samples in a period of reference voltage. The choice of the repetitive controller gain must ensure a good transient response and the stability of overall closed-loop system. Higher repetitive controller gain results in fast convergence of the output error, however the feedback system may become unstable for high values of c_1.

Then, the resulting control law $u(k)$ becomes:

$$u(k)=u_{OSAP}(k)+u_{RP}(k) \quad (14)$$

IV. Predictive PD-Feedforward Controller with Repetitive Integral Action

The classic PID controller has been used in many industrial control systems, principally because of its simple structure that can be easily understood and implemented in practice, and its excellent flexibility made possible by adjustment of the coefficients K_P, K_I and K_D. The equation of the PID controller in the continuous-time domain is:

$$u_{PID}(t)=K_Pe(t)+K_I\int e(t)dt+K_D\frac{de(t)}{dt} \quad (15)$$

For a microcontroller implementation, (15) becomes

$$u_{PID}(k)=K_Pe(k)+K_IT\sum_{n=1}^{k}e(n)+\frac{K_D}{T}[e(k)-e(k-1)] \quad (16)$$

According to (16), the control variable $u_{PID}(k)$ depends upon the present value and the previous values of the output error $e(k)$. If the required computation time to implement $u_{PID}(k)$ is not small, there may be benefit in predicting the value of $e(k)$ at time $t = (k-1)T$, and then computing $u_{PID}(k)$ from (16).

In this way, a simple linear prediction algorithm can be used to predict the output error $e(k)$ [11], [12], that is:

$$e(k)=e(k-1)+[e(k-1)-e(k-2)] \quad (17)$$

Using (17) to predict $e(k)$ in (16), the predictive PID controller equation becomes:

$$\begin{aligned} u_{PID}(k)&=\left[2K_P+2K_IT+K_D/T\right]e(k-1)\\ &-\left[K_P+K_IT+K_D/T\right]e(k-2)+\left[K_IT\right]\sum_{n=1}^{k-1}e(n) \end{aligned} \quad (18)$$

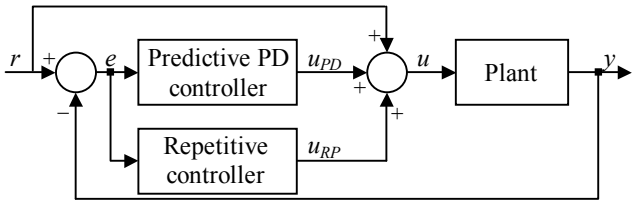

Fig. 5. Block diagram of the control system with predictive PD-feedforward controller with repetitive integral action.

To reduce the output error for linear and nonlinear cyclic loads, a feedforward action and a repetitive controller are added to predictive PID controller [9], as shown in Fig. 5.

Consequently, due to inclusion of the repetitive controller with integral action along with the control law, it is possible to eliminate the integral action from the PID controller. Thus, the computational effort for the controller implementation is reduced without affecting system performance. By removing the integration from the predictive PID controller, (18) becomes,

$$u_{PD}(k) = K_1 e(k-1) + K_2 e(k-2) \tag{19}$$

where

$$\begin{aligned} K_1 &= 2K_P + K_D/T \\ K_2 &= -K_P - K_D/T \end{aligned} \tag{20}$$

Then, the control law $u(k)$ becomes:

$$u(k) = u_{PD}(k) + u_{RP}(k) + r(k) \tag{21}$$

In [9], predictive PD-feedforward controller gains (K_1 and K_2) are determined by allocating the two dominant poles of the closed-loop system, such that the feedback system with repetitive controller has a good performance for any resistive load.

V. Model Reference Controller with Repetitive Integral Action

Consider a single-input single-output plant as presented in Fig. 6. The input $u(k)$ and output $y(k)$ signals are used to generate $m-1$ dimensional auxiliary vectors, ω_1 and ω_2 respectively, where m is the order of the system to be controlled. Such that,

$$\begin{aligned} \omega_1(k+1) &= F\,\omega_1(k) + q\,u(k) \\ \omega_2(k+1) &= F\,\omega_2(k) + q\,y(k) \end{aligned} \tag{22}$$

where F is a stable matrix and (F,q) is a controllable pair.

As defined in [13], (F,q) is the state space realization of $\alpha(z)/\Lambda(z)$, i.e.,

$$(z-F)^{-1} q = \frac{\alpha(z)}{\Lambda(z)} \tag{23}$$

The polynomial $\Lambda(z)$ is chosen as being monic, Hurwitz of degree $m-1$ and its poles must be matched with the dynamics of the reference model as well as with the dynamics of the known part (nominal model) of the plant.

In this case, the control law is given by:

$$u_{MRC}(k) = \boldsymbol{\theta}^T \boldsymbol{\omega}(k) + c_o r(k) \tag{24}$$

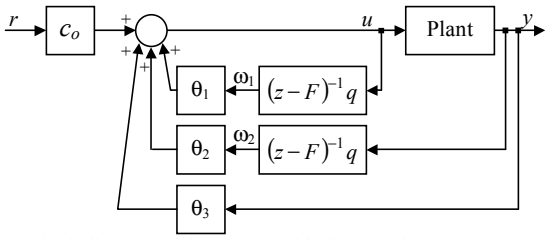

Fig. 6. Block diagram of the system with the model reference controller.

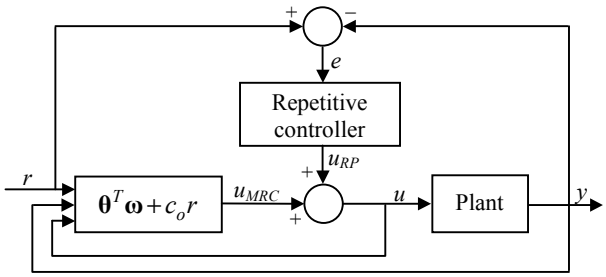

Fig. 7. Block diagram of the control system with the model reference controller with repetitive integral action.

where $\boldsymbol{\theta}^T = [\theta_1 \;\; \theta_2 \;\; \theta_3]$ is a $(2m-1)$ dimensional control parameters vector tuned *a priori* using a robust model reference adaptive controller (RMRAC), which uses a modified least-squares adaptation algorithm [7], [10]. Furthermore, $\boldsymbol{\omega}^T(k) = [\omega_1(k) \;\; \omega_2(k) \;\; y(k)]$ is a vector containing the auxiliary states $\omega_1(k)$ and $\omega_2(k)$ and the output $y(k)$, and c_o is a feedforward gain.

Again, a repetitive controller is added to model reference controller, as shown in Fig. 7, to reduce the steady-state error and periodic errors caused by periodic disturbances.

The control law $u(k)$ then becomes:

$$u(k) = u_{MRC}(k) + u_{RP}(k) \tag{25}$$

VI. Stability Analysis

The absolute stability of the feedback systems has been investigated by the localization of the closed-loop poles with the variation of the plant parameters (R, L and C).

Fig. 8 shows the stability region of the predictive OSAP controller in $\omega_p\zeta_p$–plane. This figure also gives the trajectories of the plant parameters in this plane. For a given trajectory, one parameter varies along the trajectory and the other two parameters are held constant at their nominal values. Fig. 8(a) shows the stability region when the predictive OSAP controller is designed with ζ_p = 0.25 and ω_p = 6325 rad/s. On the other hand, if a MPWM pattern is used, it is possible to reduce the output filter parameters and, consequently, to design the predictive OSAP controller for a higher natural frequency. By using a MPWM pattern with three voltage pulses per sampling period, the predictive OSAP controller is designed with ζ_p = 0.25 and ω_p = 11550 rad/s, and stability region is shown in Fig. 8(b). It can be seen that with the appropriate design of the predictive OSAP controller the stability margin of the closed-loop system increases and, then, its performance can be improved.

Fig. 9(a) presents the stability region of the predictive PD-feedforward controller, when the switching frequency is equal to the sampling frequency (10.8 kHz). Thus, the natural frequency of the output filter is ω_p = 6325 rad/s. Fig. 9(b) shows the stability region of the predictive PD-feedforward controller, when a MPWM pattern with three voltage pulses per sampling period is used for a natural frequency of the output filter equal to ω_p = 11550 rad/s. In the same way, Fig. 10 shows the stability region of the model reference controller in $\omega_p\zeta_p$–plane. From Fig. 9 and Fig. 10, it is possible to verify that the predictive PD-feedforward controller and the model reference controller are less sensitive to parametric variations if compared with the predictive OSAP controller.

Thus, considering that the closed-loop systems without the repetitive control action are stable for a large range of plant parameters, as can be seen in Fig. 8(b) to Fig. 10, the stability of the systems is determined by the repetitive controller. In [8], [9] and [10], the stability analysis with repetitive controller was carried out. Therefore, demonstrating that the control systems shown in Fig. 4, Fig. 5 and Fig. 7 are stable.

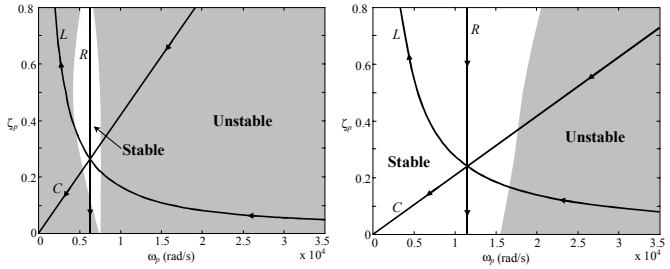

Fig. 8. Stability region of predictive OSAP controller in $\omega_p\zeta_p$-plane. (a) Nominal values: C = 25 μF, L = 1 mH and R = 12 Ω. (b) Nominal values: C = 15 μF, L = 0.5 mH and R = 12 Ω.

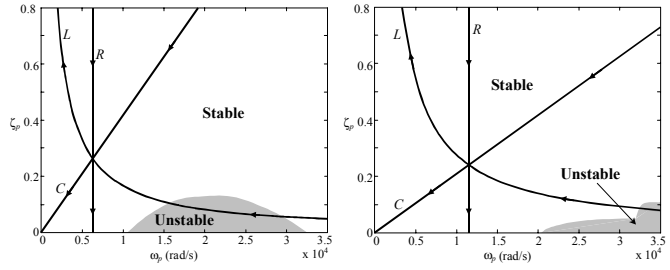

Fig. 9. Stability region of predictive PD-feedforward controller in $\omega_p\zeta_p$-plane. (a) Nominal values: C = 25 μF, L = 1 mH and R = 12 Ω. (b) Nominal values: C = 15 μF, L = 0.5 mH and R = 12 Ω.

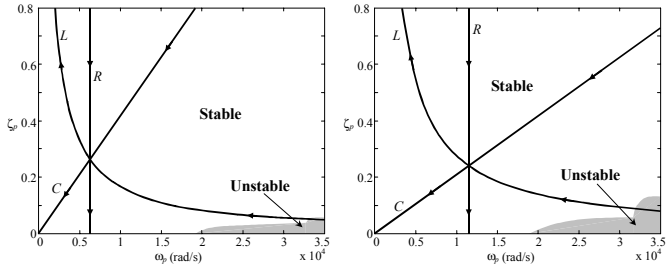

Fig. 10. Stability region of model reference controller in $\omega_p\zeta_p$-plane. (a) Nominal values: C = 25 μF, L = 1 mH and R = 12 Ω. (b) Nominal values: C = 15 μF, L = 0.5 mH and R = 12 Ω.

VII. Simulation Results

Table I gives the parameters of the single-phase full-bridge PWM inverter system used in digital computer simulation (with MATLAB®) to verify the performance of the digital control schemes presented in the previous sections. The parameters of these controllers for a PWM pattern with one voltage pulse in the beginning of the sampling period and for a MPWM pattern with three voltage pulses per sampling period are presented in Table II.

TABLE I
Parameters of PWM Inverter

Output filter I	L = 1 mH
(Switching frequency = 10.8 kHz)	C = 25 μF
Output filter II	L = 0.5 mH
(Switching frequency = 32.4 kHz)	C = 15 μF
DC input voltage	V_B = 200 V
Reference voltage	r = 110 V_{RMS}, f = 60 Hz
Nominal resistive load	R = 12 Ω
Sampling frequency	f_S = 10.8 kHz
Sampling period	T = 92.6 μs

TABLE II
Parameters of the Controllers

Controller	PWM Pattern	MPWM Pattern
Predictive OSAP controller	P_1 = –1.3614 P_2 = 1.0633 Q_1 = 0.2785 Q_2 = 0.4032 Q_3 = 0	P_1 = –0.0196 P_2 = 0.4698 Q_1 = 0.5561 Q_2 = 0.6843 Q_3 = 0.1944
Predictive PD-feedforward controller	K_1 = 0.1033 K_2 = –0.2523	K_1 = –0.199 K_2 = –0.029
Model reference controller	$\boldsymbol{\theta}^T$ = [–13.75 14.32 0] c_o = 1 q = 0.008 F = 0.7344	$\boldsymbol{\theta}^T$ = [–34.82 35.21 0] c_o = 1 q = 0.0072 F = 0.5979
Repetitive controller	c_1 = 0.2	c_1 = 0.2

A. PWM pattern with one voltage pulse in the beginning of the sampling period

Initially, the predictive OSAP controller with repetitive control action (OSAP-RP) was simulated using a PWM pattern with one pulse in the beginning of the sampling period. Fig. 11 shows the output voltage $v_c(t)$ waveform for nominal resistive load (12 Ω).

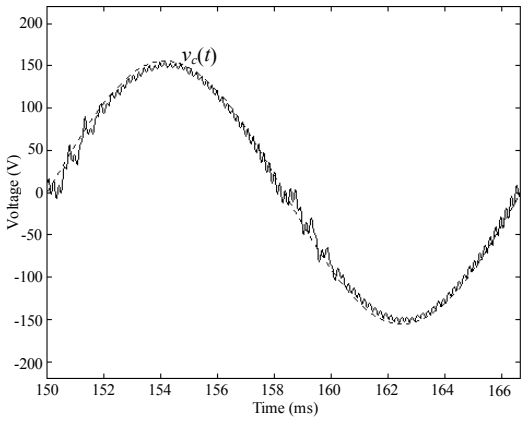

Fig. 11. Response of the OSAP-RP for nominal load, using a PWM pattern with one pulse in the beginning of the sampling interval.

Due to simplifications realized to obtain a linear discrete-time model, and considering the design methodology employed to determine the output filter parameters, it can be observed that the predictive OSAP controller with repetitive integral action does not perform well when this PWM pattern is used. With these output filter parameters, the control signal presented undesired oscillations, causing a degradation of the output voltage waveform [8]. In addition, the closed-loop system became unstable for no-load, as shown in Fig. 12.

Consequently, only the predictive PD-feedforward controller with repetitive integral action (PD-RP) and the model reference controller with repetitive integral action (MRC-RP) were simulated under nonlinear loads with this PWM pattern. Simulation results obtained for these two controllers are similar, as can be seen in Fig. 12 to Fig. 14, because these controllers have been designed from similar specifications. Fig. 12 shows the THD of the output voltage waveform for nominal load and no-load. On the other hand, Fig. 13 presents a comparison of the simulation results obtained for nominal resistive load in series with a Triac, with different firing angles, to verify the performance of these controllers for ac phase-controlled loads. Finally, Fig. 14 shows the THD of the output voltage waveform for a rectifier load (with a current crest factor of 2.5), to demonstrate the performance of these controllers for this type of load.

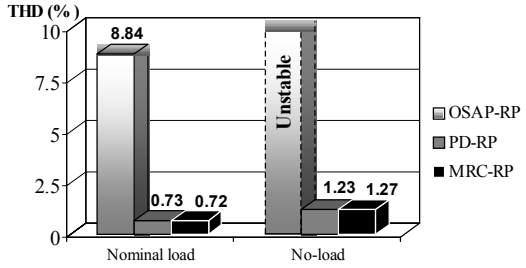

Fig. 12. THD of the output voltage for linear loads, using a PWM pattern with one voltage pulse in the beginning of the sampling interval.

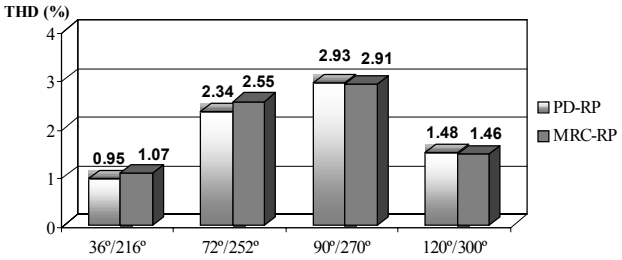

Fig. 13. THD of the output voltage for nonlinear loads, using a PWM pattern with one voltage pulse in the beginning of the sampling interval.

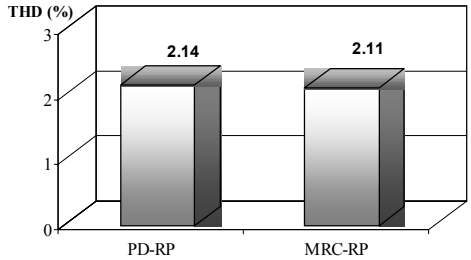

Fig. 14. THD of the output voltage for a rectifier load, using a PWM pattern with one voltage pulse in the beginning of the sampling interval.

B. MPWM pattern with three voltage pulses per sampling period

It was demonstrated in Section II that the plant modeling errors caused by the linearization of the discrete-time plant model become smaller as the number of voltage pulses per sampling period increases. Therefore, the switching frequency was increased to 32.4 kHz (maximum frequency allowed by the used microcontroller with an 8-bit resolution) while the sampling frequency was maintained the same. With this, the output filter parameters could be reduced to improve the performance of the predictive OSAP controller [8].

Fig. 15 shows a comparison of the THD for nominal load and no-load. In addition, to verify the performance of these controllers with fixed-point routines, Fig. 16 presents a comparison of the simulation results obtained for nominal load with double precision floating-point routines (1-bit of signal, 11-bits of exponent and 52-bits of mantissa) and with fixed-point routines (8-bits). This figure shows that the model reference controller with repetitive integral action presented the superior performance with fixed-point routines among these techniques. On the other hand, Fig. 17 presents a comparison for nominal resistive load in series with a Triac, with different firing angles, to verify the performance of these controllers for cyclic loads. The predictive PD-feedforward controller and the model reference controller, both with the inclusion of the repetitive control, presented a similar performance, while the predictive OSAP controller with repetitive integral action presented a higher THD.

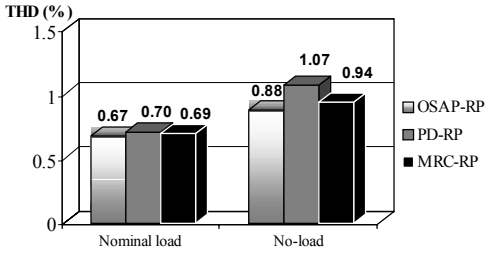

Fig. 15. THD of the output voltage for linear loads, using a MPWM pattern with three voltage pulses per sampling period.

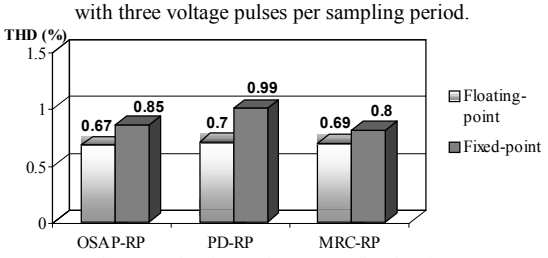

Fig. 16. Floating-point *versus* fixed-point.

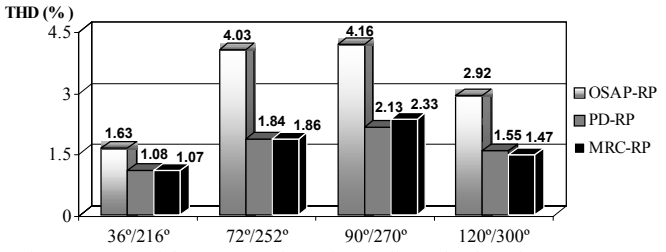

Fig. 17. THD of the output voltage for nonlinear loads, using a MPWM pattern with three voltage pulses per sampling period.

Fig. 18 shows the influence of the repetitive integral action for input and output periodic disturbances. Fig. 18(a) presents the convergence of THD for nominal resistive load in series with a Triac commuting at 72º/252º (periodic output disturbance). Although the THD of the output voltages are similar at the first cycle, it can be seen that the THD of the output voltages by using the predictive PD-feedforward controller or the model reference controller, both with repetitive control, are less than by using the predictive OSAP controller with repetitive control. On the other hand, Fig. 18(b) presents the convergence of THD when the dc bus voltage presents 120 Hz ripple with amplitude of ±15% of the input nominal voltage (periodic input disturbance), which could be caused by a front-end preregulator converter connected to the utility grid. Again, it is possible to observe that the repetitive integral action minimizes the THD of the output voltage, however the output voltage waveform presented a higher THD by using the predictive OSAP controller. Consequently, the repetitive controller gain c_1 should be higher for the predictive OSAP controller with repetitive action to synthesize an output voltage with low THD for input and output periodic disturbances. If the repetitive controller gain c_1 is increased, the convergence of the output error will be faster, however the feedback system may become unstable. In this way, the choice of c_1 is a compromise between the relative stability of the closed-loop system and the convergence rate of the output error [6].

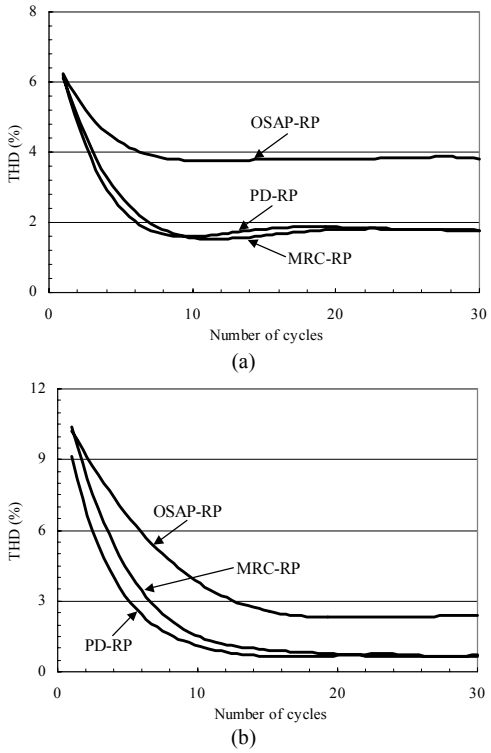

Fig. 18. Influence of the repetitive integral action for a periodic disturbance (c_1 = 0.2). (a) Nominal resistive load in series with a Triac commuting at 72º/252º (output disturbance). (b) DC bus voltage containing 120 Hz ripple with amplitude of ±15% of the input nominal voltage (input disturbance).

VIII. Experimental Results

A laboratory prototype of the single-phase PWM inverter using IGBT's has been built to verify the real performance of the controllers analyzed in this paper. The component values of the inverter system and the parameters of the controllers are the same as those used in the simulation (Tables I and II).

The controllers have been implemented using an eight bits wide data word microcontroller (PIC17C756 of Microchip Technology Inc.). It has an embedded 10-bit A/D converter and a PWM signal generator. Table III shows the execution time of the control algorithms implemented with PIC17C756 microcontroller. The execution time (output voltage A/D conversion time and control law computation) spent by the PIC17C756 does not allow to increase the sampling frequency, however the PWM signal frequency can be equal to 32.4 kHz with an 8-bit resolution.

TABLE III
Execution Time of the Algorithms

Controller	Execution time
Predictive OSAP controller with repetitive control action	65 µs
Predictive PD-feedforward controller with repetitive control action	60 µs
Model reference controller with repetitive control action	72 µs

A. PWM pattern with one voltage pulse in the beginning of the sampling period

Fig. 19 shows a comparison of the experimental results obtained for nominal resistive load and no-load. Due to the fact that the predictive OSAP controller with repetitive integral action became unstable for no-load in simulations, only the other two controllers were implemented under no-load and nonlinear cyclic loads. Fig. 20 presents a comparison of the experimental results obtained for a rectifier load with a current crest factor of 2.5. Fig. 21 presents the response of the model reference controller with repetitive integral action for this rectifier load, which presented the superior performance for this load.

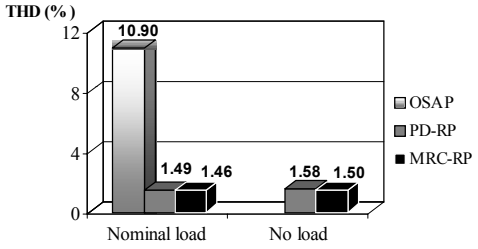

Fig. 19. Experimental results obtained for nominal load and no-load, using a PWM pattern with one pulse in the beginning of the sampling period.

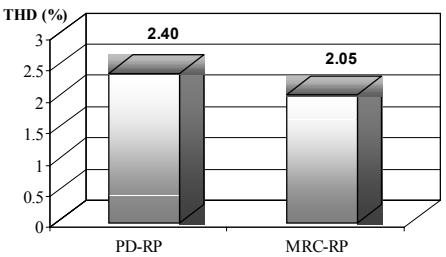

Fig. 20. Experimental results obtained for a rectifier load, using a PWM pattern with one voltage pulse in the beginning of the sampling interval.

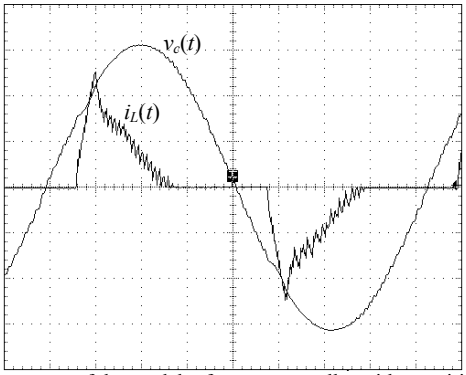

Fig. 21. Response of the model reference controller with repetitive integral action for a rectifier load, using a PWM pattern with one voltage pulse in the beginning of the sampling interval (50 V/div, 10 A/div, 2 ms/div).

B. MPWM pattern with three voltage pulses per sampling period

Fig. 22 presents a comparison of the experimental results obtained for nominal load and no-load with a MPWM pattern with three voltage pulses per sampling period. Fig. 23 shows the THD of the experimental results obtained for a rectifier load. The predictive OSAP controller presented a better performance with the reduction of the output filter parameters, which has been made possible with the use of a MPWM pattern. However, as discussed in previous section, the repetitive controller gain c_1 should be higher for the OSAP-RP controller to synthesize an output voltage with low THD for cyclic loads. On the other hand, the predictive PD-feedforward controller and the model reference controller, both with repetitive action, presented a similar performance (in terms of THD) to that obtained with a PWM pattern.

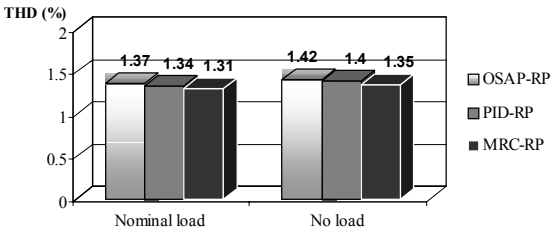

Fig. 22. Experimental results obtained for nominal load and no-load with a MPWM pattern with three voltage pulses per sampling period.

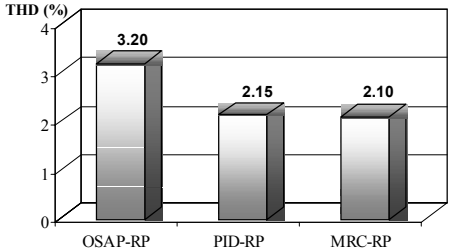

Fig. 23. Experimental results obtained for a rectifier load with a MPWM pattern with three voltage pulses per sampling period.

IX. CONCLUSIONS

This paper presents a comparison among digital control techniques with repetitive integral action applied to low cost UPS. As a result of the repetitive action, these digital control schemes can reduce the steady-state error and distortions caused by periodic disturbances. In addition, the digital control techniques analyzed measure only the output voltage, decreasing the amount of sensors and the overall system cost.

Results show that the performance of the predictive OSAP controller depends on the accuracy of the discrete-time plant model and parameters of the output filter. However, it was demonstrated that the increase of the switching frequency reduces the effects of the plant modeling errors caused by linearization of the discrete-time plant model. As the switching frequency is increased, the output filter parameters can be reduced, decreasing weight, volume and cost of the system, as well as improving enormously the performance of the closed-loop system with the OSAP-RP controller. In addition, as the sampling frequency is maintained the same, it is possible to implement this controller in a low-cost microcontroller or DSP.

On the other hand, the predictive PD-feedforward controller and the model reference controller, both with the inclusion of the repetitive integral action, are less sensitive to parametric variations if compared with the predictive OSAP controller, and presented a good performance for linear and nonlinear loads. However, among the analyzed control techniques, the model reference controller presented a superior performance with fixed-point routines.

REFERENCES

[1] A. Kawamura, T. Haneyoshi and R. G. Hoft, "Deadbeat controlled PWM inverter with parameter estimation using only voltage sensor", *IEEE Trans. Power Electr.*, v. 3, pp. 118-125, Apr. 1988.

[2] S. L. Jung and Y. Y. Tzou, "Discrete sliding-mode control of a PWM inverter for sinusoidal output waveform synthesis with optimal sliding curve", *IEEE Trans. Power Electr.*, v. 11, pp. 567-577, Jul. 1996.

[3] S. Hara, Y. Yamamoto, T. Omata and M. Nakano, "Repetitive control system: A new type servo system for periodic exogenous signals", *IEEE Trans. Autom. Control*, v. 33, pp. 659-667, Jul. 1988.

[4] T. Haneyoshi, A. Kawamura and R. G. Hoft, "Waveform compensation of PWM inverter with cyclic fluctuating loads", *IEEE Trans. Ind. Appl.*, v. 24, pp. 582-588, Jul./Aug. 1988.

[5] Y. Nishida and T. Haneyoshi, "Predictive instantaneous value controlled PWM inverter for UPS", in *IEEE Power Electr. Spec. Conf. Rec.*, 1992, pp. 776-783.

[6] Y. Y. Tzou, R. S. Ou, S. L. Jung and M. Y. Chang, "High-performance programmable AC power source with low harmonic distortion using DSP-based repetitive control technique", *IEEE Trans. Power Electr.*, v. 12, pp. 715-725, Jul. 1997.

[7] H. A. Gründling, E. G. Carati and J. R. Pinheiro, "A robust model reference adaptive controller for UPS applications", in *IEEE Ind. Electr. Conf. Rec.*, 1997, pp. 901-905.

[8] C. Rech, H. Pinheiro, H. A. Gründling, H. L. Hey and J. R. Pinheiro, "Improved modified OSAP controller for voltage source PWM inverters", in *Brazilian Power Electr. Conf. Proc.*, 2001, pp. 329-334.

[9] C. Rech, H. Pinheiro, H. A. Gründling, H. L. Hey and J. R. Pinheiro, "Analysis and design of a repetitive predictive-PID controller for PWM inverters", in *IEEE Power Electr. Spec. Conf. Rec.*, 2001, pp. 2531-2537.

[10] C. Rech, H. A. Gründling and J. R. Pinheiro, "A modified discrete control law for UPS applications", in *IEEE Power Electr. Spec. Conf. Rec.*, 2000, pp. 1476-1481.

[11] C. L. Phillips and J. M. Parr, "Robust design of a digital PID predictor controller", *IEEE Trans. Ind. Electr.*, v. 31, pp. 328-332, Nov. 1984.

[12] J. H. Aylor, R. L. Ramey and G. Cook, "Design and application of a microprocessor PID predictor controller", *IEEE Trans. Ind. Electr. and Control Instrum.*, v. 27, pp. 133-137, Aug. 1980.

[13] P. A. Ioannou and J. Sun, *Robust Adaptive Control*. Upper Saddle River, NJ: Prentice-Hall, 1996, pp. 333-372.